Vietnam Journal of Earth Sciences, 45(3), 271-286, https://doi.org/10.15625/2615-9783/18408

**Vietnam Journal of Earth Sciences**
https://vjs.ac.vn/index.php/jse

# The late Pleistocene - Holocene sedimentary evolution in the Ba Lat River mouth area of the Red River Delta

Tran Ngoc Dien[1], Vu Van Ha*[2,3], Amelie Paszkowski[4], Nguyen Minh Quang[2], Ngo Thi Dao[2], Nguyen Thi Min[2], Dang Xuan Tung[2], Nguyen Chi Dung[2], Vu Ngoc Tuyen[1], Nguyen Khanh Tung[1], Tran Ngoc Huan[1]

[1]*Department of Marine Geology and Minerals - General Department of Geology and Minerals of Vietnam, Hanoi, Vietnam*
[2]*Institute of Geological Sciences, VAST, Hanoi, Vietnam*
[3]*Graduate University of Science and Technology, VAST, Hanoi, Vietnam*
[4]*Environmental Change Institute, University of Oxford, UK*

Received 18 October 2021; Received in revised form 17 April 2023; Accepted 5 June 2023

ABSTRACT

The Ba Lat estuary is part of the downstream stretch of the Red River Delta, the second-largest Delta in Vietnam and the 12th largest in the world. This study analyses GAT borehole sediments in the Ba Lat estuary area to assess environmental changes during the Late Pleistocene - Holocene period. This entailed detailed analyses of 70 m-deep borehole data from the Ba Lat estuary area, including structural analysis of 70 m-deep sediment core samples, 230 samples of grain size, 49 samples of Foraminifera, five samples of petrographic thin slices, and four samples of radiocarbon dating.

The data reveal nine sedimentary facies, including river channel sand facies, floodplain clayey silt facies, tidal flat sandy-silty facies, bay clayey silt facies, pro-delta clayey silt facies, delta front sandy-silty clay facies, mouth bar sand facies, tidal flat sandy - silty clay facies, and delta plain silty clay facies. The combined nine sedimentary facies formed sequentially in time, representing the evolution of the sedimentary environment from the Late Pleistocene to the Holocene and the evolutionary process from the continental to the estuarine and Delta environment.

The results also enable the geographic identification and delineation of the incised valley in the Red River Delta during the Late Pleistocene to Holocene period. The sedimentation rate in the incised valley varies from period to period. In the sedimentation phase of the incised valley, the average accretion rate reached 11.64 mm/year. In contrast, during the open sea regime (shallow sea near the coast), the accretion rate was observed to be very low, with a rate of 1.27 mm/year and the period of delta formation had the highest accretion rate, reaching 13.41 mm/year.

*Keywords*: Red River Delta, Late Pleistocene - Holocene, sedimentary facies, incised valley.

## 1. Introduction

Human activities and natural hazards like erosion, sea level rise, volcanoes, salinization, heavy metals, microplastics, and Arsenic pollution currently impact the environment. Many events are revealed from the Quartenay sediments (Hoan et al., 2022, Doan Thi et al., 2021, Le et al., 2022, Le Duc et al., 2022, Hoang Van et al., 2022).

*Corresponding author, Email: vuha@igsvn.vast.vn

The Red River Delta (or the Northern Delta) is located in northern Vietnam and is the 12th largest river delta in the world. It is dominated by tides and waves, with a spring tidal range of 3.2 m and a sediment load of 130 million tons/year (Fan, 2012; Milliman and Syvitski, 1992). The results of sea level monitoring in this area show that the sea level has been gradually increasing between 1960 and 2020 (21.4 cm) (Hai et al., 2022). The study area has a tropical climate, and precipitation is mainly concentrated during the rainy season (80% of the total annual rainfall) (Luu and Hien, 2022).

The Red River Delta plain revealed that sediments at these sites could be classified into three units: fluvial sediments, estuarine sediments, and deltaic sediments (Tanabe et al., 2003a, 2003b, 2006; Duong et al., 2020). The estuarine sediments and the deltaic sediment are widely distributed across the Red River Delta. The sedimentary facies are divided into boreholes such as ND1, DT, VN, HV, NB, GA (Tanabe et al., 2003a, 2003b, 2006), CC borehole (Hori, 2004), NP borehole (Duong, 2009), DA, PD, TL boreholes (Funabiki et al., 2007), TS, PN boreholes (Nghi and Toan, 2000), and HH120 borehole (Lam and Boyd, 2001). However, the distribution of fluvial sediments in the incised valley is not widespread, and only a small number of boreholes, such as ND1 and NP, have detected these.

The Pleistocene - Holocene incised valley in the Red River Delta contains essential information about how the Delta evolved and its sedimentary environment. Previous studies, including those by Thanh et al. (2018), used high-resolution shallow seismic data to identify and delineate incised valleys. However, there is little research on sedimentary evolution, especially the incised valley sedimentation. Articles referring to the incised valley as well as its direction, are attested to by boreholes. Therefore, the delineation of the incised valley is still lacking information. The GA borehole (40.2 m depth) in Ba Lat was performed by (Tanabe et al., 2006) and identified two sedimentary units (estuarine sediments and deltaic sediments). The GAT borehole was conducted near the GA borehole with a greater depth (70 m depth) to add information about sedimentary facies, especially locating the incised valley.

## 2. Materials and Methods

This article presents new results based on 70 m deep, continuous core samples taken in the Ba Lat estuary area in the Giao An commune, Giao Thuy district, Nam Dinh province (coordinates X: 106°30'48.00"E, Y: 20°15'40"N, Z: +1.1 m) (Fig. 1). The sediment core was extracted using a rotary drilling machine, and the intact sample was subsequently transferred to the laboratory. The sample was split in half, enabling the description and composition of the type and structure of sediment, including the sedimentary layers and the variation in the sedimentary spans, as well as the vegetation and shell remnants, to understand traces of biological activity. The microstructures were identified on X-Ray images by X-ray irradiation, and images were obtained.

### *2.1. Grain size analysis method*

Using the Particle LA-960 laser scattering particle size distribution analyzer, the grain size was divided according to the Wentworth (1922) scale of sand from 2-0.063 mm, silt from 0.063-0.0039 mm, and clay less than 0.0039 mm. Two hundred and thirty samples were collected along the core, with 1 sample at 20-50 cm intervals. The results are shown on a graph of grain size distribution along the core with the parameters such as particle size composition, sorting, and mean grain size.

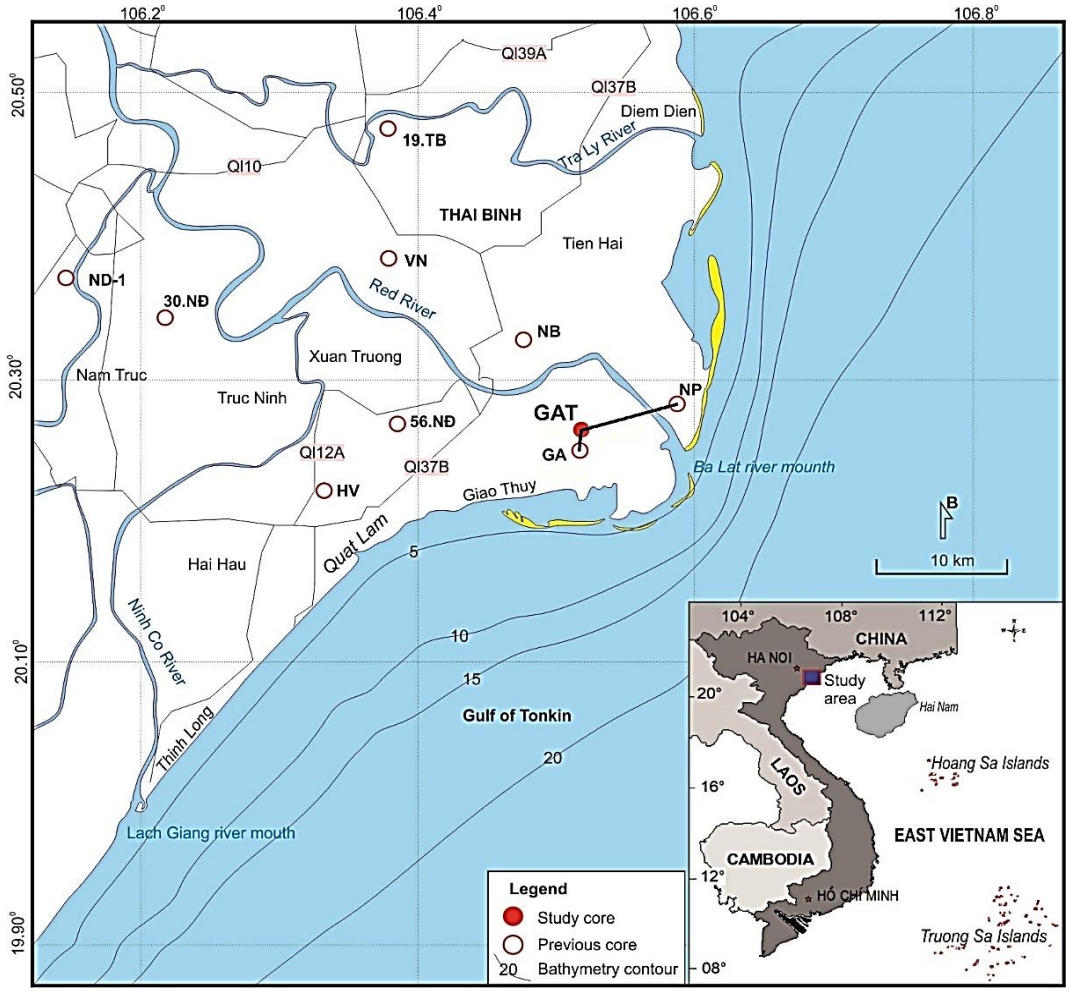


*Figure 1*. Borehole location and study area

### *2.2. Foraminifera analysis method*

Foraminifera fossils were analyzed on Euromex stereo microscopes at magnifications of x10, x20, and x40 at the Institute of Geological Sciences - Vietnam Academy of Science and Technology laboratory. This enabled species classification based on materials and methods developed by Jean Piere Debenay et al., 1998, 2012; Nguyen Ngoc, 2006; Ma Van Lac et al., 2009; and Yanli Lei and Tiegang Li, 2016. Specimens for analysis of Foraminifera fossils were collected with 49 samples along the core from 1 m to 49 m, 1 sample at 1m intervals. The analyzed results are shown on a chart divided into 4 Foraminifera Paleozoic zones based on richness, number of species, or discontinuity (no fossils).

### *2.3. Petrographic thin section analysis method*

The petrographic thin section method was applied to determine the mineral composition in loose sediments and the particle size, selectivity, and roundness. This informed the naming and explaining of sediment formation, The selected sediments for analysis are coarse to medium-grained sand sediments, and 5 samples were taken.

### *2.4. $^{14}C$ dating method*

Sediment samples, including carbonate shell fragments and plant humus, were processed and analyzed at Lab Direct AMS, USA. These results were calibrated using Calib Rev 8.1.0 software for marine origin samples corrected by Marine20 (Stuiver and Reimer, 2020), and continental samples were corrected by IntCal20 (Reimer et al., 2020). A total of 4 samples were analyzed.

## 3. Results

The evolution of the sedimentary environment in the study area is shown by sedimentary facies based on sedimentary structure observation, grain size analysis, Foraminifera, and 14C dating of samples.

### *3.1. Incised valley facies F1*

#### *3.1.1. River channel sand facies F1.1*

McGowen and Gamer (1970) examined modern and ancient coarse-grained point bars. River channel sediments may encounter wood fragments, bones, or other materials (Richard, 1992).

River channel sediments are distributed across the boreholes at 54.5 m and 70 m depths. These facies are characterized by grade bedding sand of coarse to fine (Fig. 4, P17), cross-bedding sand, and silty sand (Finger 4, P18). The sedimentary parameters consist of mean grain size (Md): 0.1-0.35 mm, moderately sorted. The analyses of lithographic thin sliced samples by Microscope at depths of 69.8 m, 66.7 m, 63.7 m, 59.7 m, and 55.7 m (Fig. 2) indicate that the material composition is mainly quartz, accounting for 50-75%, as well as feldspar (1-3%), mica (3-7%), and rock fragments (15-32%), of medium to good roundness and moderately to well sorted upward trend. Some wood fragments occurred at a depth of 69.47-69.51 m. The $^{14}C$ dating of 12,870 years BP at the 69.51 m depth (Table 1).

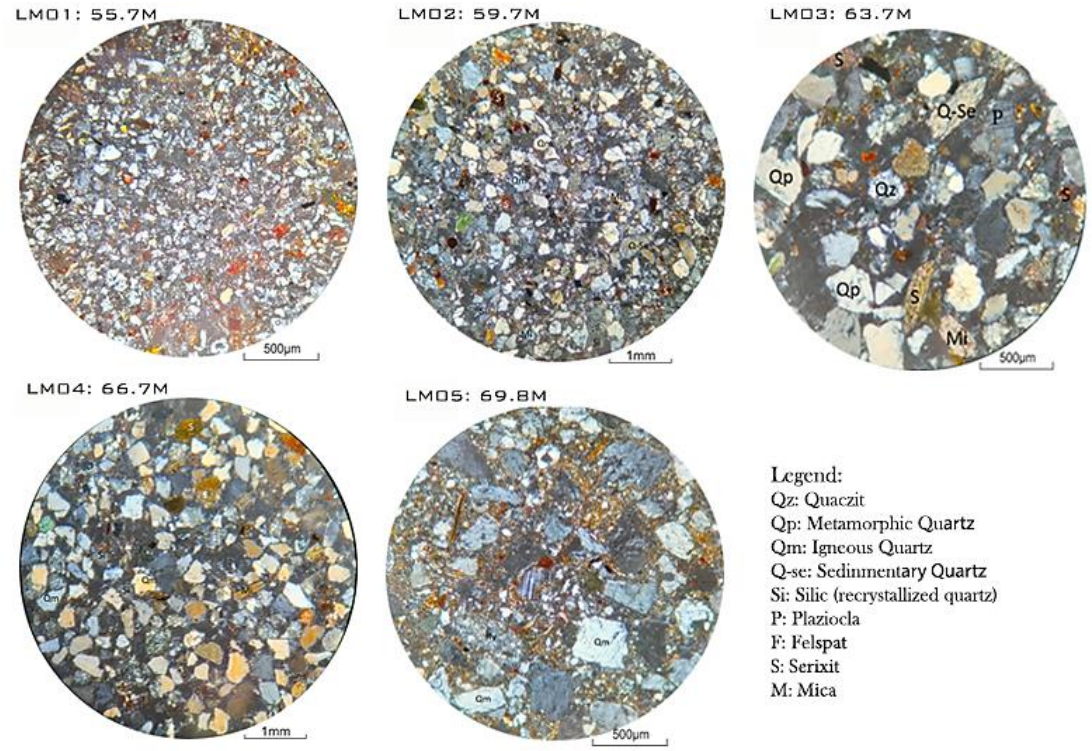


*Figure 2*. Sediment samples under a Microscope in the GAT borehole

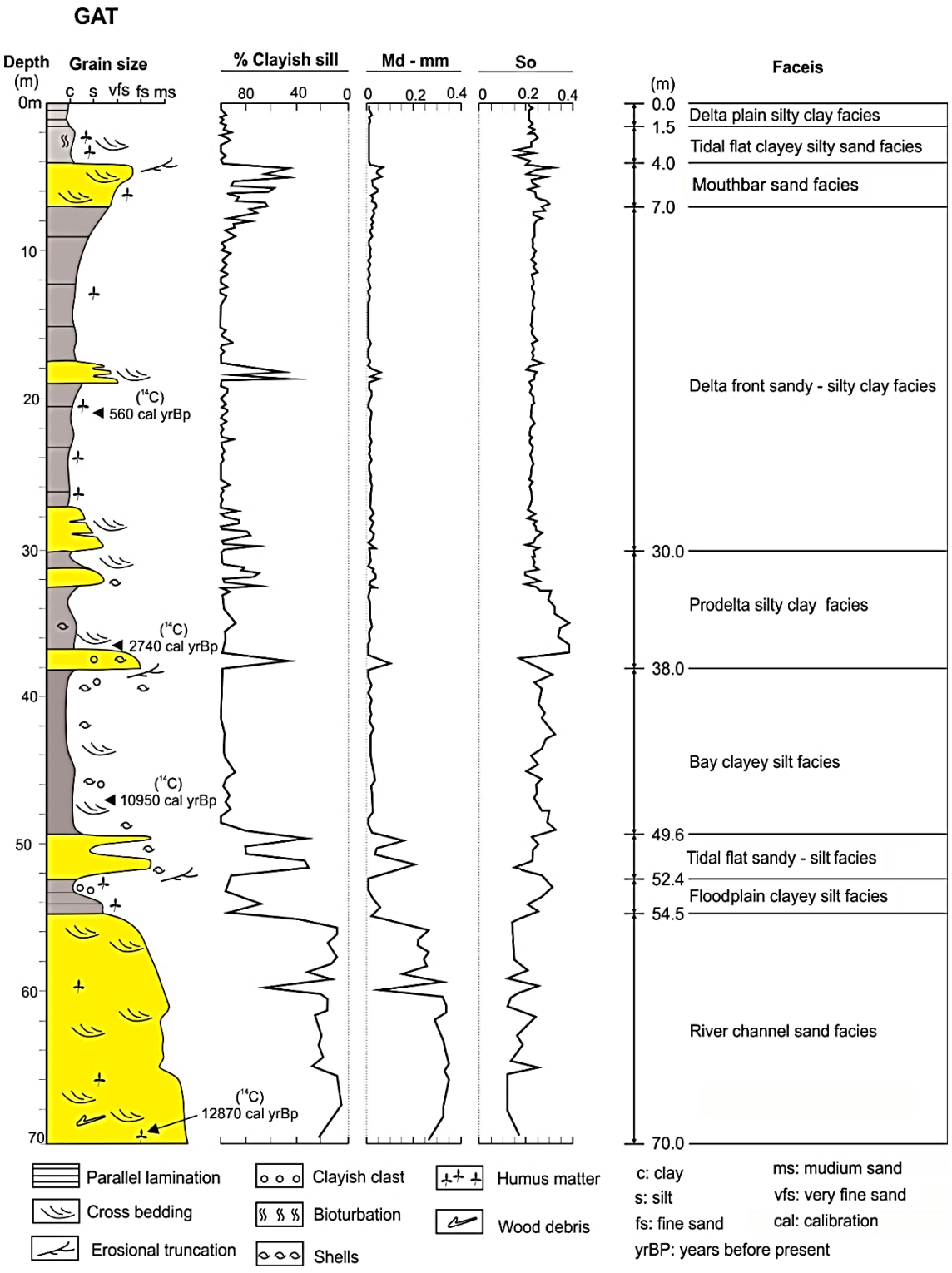


*Figure 3*. Sedimentary facies in the GAT borehole

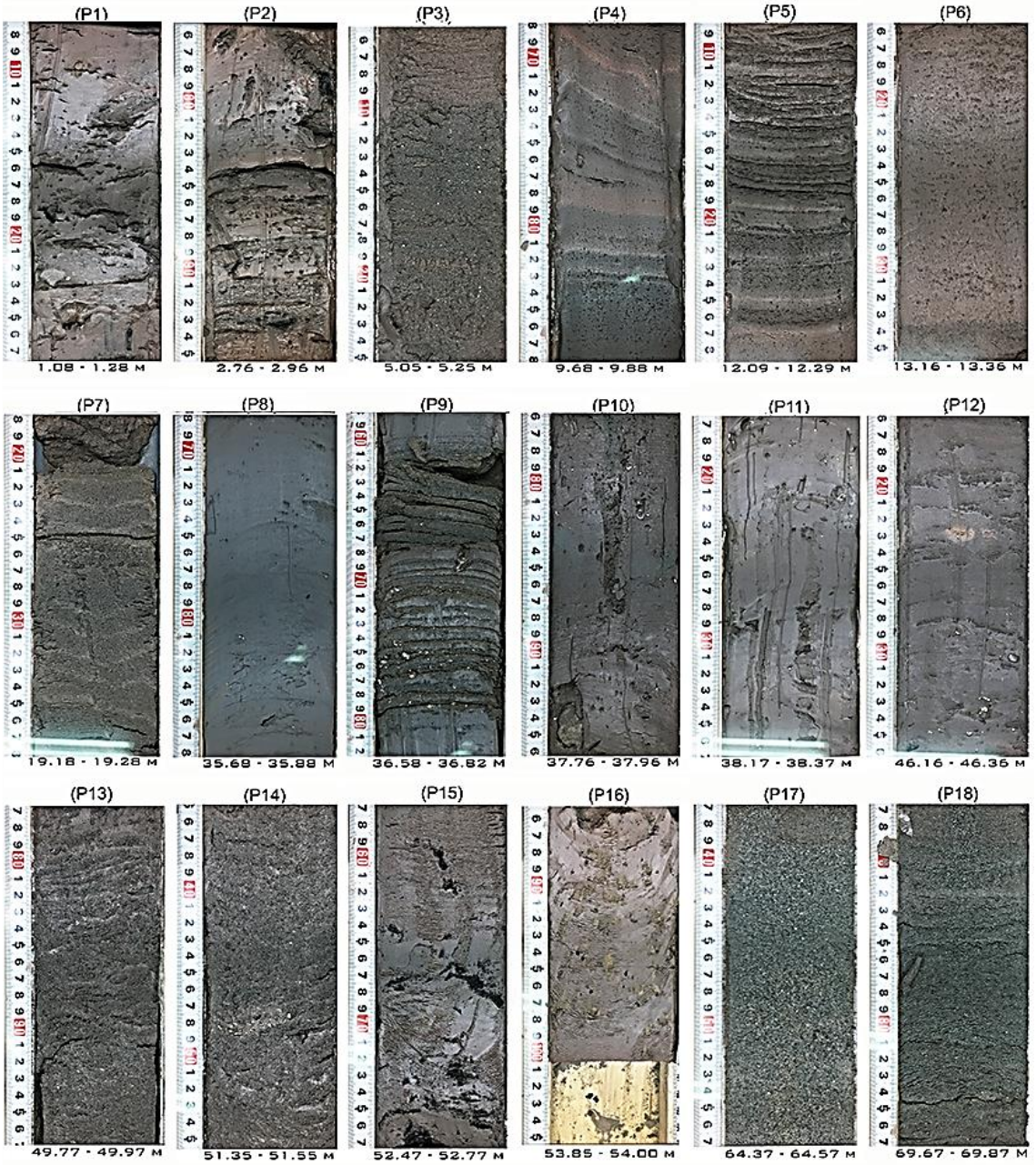


*Figure 4.* Sample GAT borehole

*Borehole legend:* P18: medium sand, cross-bedding; P17: medium to fine sand, grade bedding; P16: laterite clayey silt; P15: clayey silt thick layered; P14: silty sand shell fragments; P13: silty sand flaser bedding; P12: clay pebbles; P11: clayey silt thick layered with shell fragments; P10: yellow clay pebbles; P9: sand parallel thin layered; P8: dark green clay thick layered; P7: fine - grain ripples parallel; P6: silty clay thick layered; P5: clayey silt and fine - grain parallel, obliquely layered and ripples; P4: silty sand parallel, obliquely layered; P3: fine - grain parallel layered; P2: silty clay and fine - grain parallel layered containing humus; and P1: clayey silt thick layered

*Table 1*. Results of Radiocarbon dating $^{14}C$ in the GAT borehole

| No | Lab sample number | Symbol | Depth (m) | Conventional Age (yrBP) | Calibrated Age (cal yrBP) | | |
|---|---|---|---|---|---|---|---|
| 1 | D-AMS 042871 | (GAT/C01) | 20,15 | 962±44 | 466 | 654 | **560** |
| 2 | D-AMS 042872 | (GAT/C02) | 36,8 | 2941±42 | 2607 | 2866 | **2740** |
| 3 | D-AMS 042873 | (GAT/C03) | 47,16 | 9894±66 | 10752 | 11149 | **10950** |
| 4 | D-AMS 042881 | (GAT/C04) | 69,51 | 10921±74 | 12742 | 12993 | **12870** |

*3.1.2. Floodplain clayey silt facies F.1.2*

A floodplain is an area of land adjacent to a stream or river which stretches from the banks of its channel to the base of the enclosing valley walls (Davis, 1992). The floodplain sediments are distributed at 52.4 - 54.5 m depth in the borehole sample. The composition consists of brown clay with a parallel horizontal layered structure and sedimentary parameters of median grain size (Md) (< 0.05) and a degree of sorting (So) of 1.5-3. At a depth of 53.8-54 m (Fig. 4, P16), the sediment contains many yellow laterite clasts (0.5-1 cm in size). The laterite clast may be transported several kilometers and deposited by floods (Li et al., 2017). Plant humus is also often observed in spots and nests scattered within the sediment, ranging in size from a few mm to 1cm; even 2 cm pieces of wood are found at a depth of 53.1 m (Fig. 4, P15).

***3.2. Estuarine facies F2***

*3.2.1. Tidal flat sandy-silt facies F2.1*

The tidal flats sediments consist of gray, fine-grained sand at 49.6-52.4 m depth, with median grain size (0.005-0.15) and a degree of sorting (So) of 1.5-2.5. This sediment has flasher bedding structures (Fig. 4, P13). Flaser bedding structures are tidal structures that belong to one of the three typical structures of intertidal sediments (Nichols, 2009). The sediment contains many shell fragments, especially at 51.5 m depth (Fig. 4, P14). Foraminifera are absent.

*3.2.2. Bay clayey silt facies F2.2*

The bay facies are distributed at a depth of 38.0-49.6 m and are mainly composed of brown clayey silt with an average particle size between 0.02 and 0.04 mm and a degree of sorting of 2-2.5. The sediment has thick, parallel, horizontal, and massive layering (Fig. 4, P11) and contains many shell fragments distributed continuously at different depths but at an average interval of 31 cm. These shell fragments have typical sizes of between 0.5 cm and 1 cm. Clay pebbles from wave and tidal erosion are also encountered at 38.5 m and 46.3 m, with a size of about 1cm (Fig. 4, P12). Analysis of 7 Foraminifera samples at depths of 38.5 m; 39.5 m; 40.5 m; 43.1 m; 44.9 m; 46.7 m, and 48.5 m was undertaken. However, no fossils were found in the sediments. The absolute Age of $^{14}C$ analysis at a depth of 47.16 m showed 10,950 years cal BP (Table 1).

***3.3. Deltaic facies F3***

*3.3.1. Prodelta silty clay facies F3.1*

These facies are distributed at depths of 32-38 m and are characterized by grayish-green, massive silty clay (Fig. 4, P8), and grayish-brown lamination sand containing many shell fragments were observed at depths from 35.35 m to 37.57 m, and depths between 36.6 and 36.8 m particles from erosion caused by waves and tides in the coastal area were observed (Fig. 4, P9). Silty clay has a mean grain size (Md) of 0.02 and 0.03 mm and a degree of sorting (So) of 2.5-3.5. Clay pebbles are scattered throughout this facies, especially at a depth of 37.95 m, where a solid yellow clay pebble with a diameter of about 2 cm was encountered (Fig. 4, P10). The $^{14}C$ dating of 2,740 cal BP at the 16.8 m depth. The sediment contains rich and diverse fossils, large and visible at the surface. Some species typically living in shallow seas relatively far from shore

were identified in the sample, such as *Pseudorotalia Indo-Pacific, Textularia foliacea,* and *Biggenerina nodosaria* (Stephen J. Gallagher et al., 2009; Reymond et al., 2014; Armon et al., 2015; Lei and Li, 2016). Fossils are less diverse and abundant at depths between 30m and 36m, particularly in the lower parts (36-38m). However, even at such depths, typical species for shallow coastal marine environments were found, such as *Hanzawaia nipponica, Cibicidoides wuellerstofi, Ammonia pauciloculata,* and *Elphidum advenum* (Nguyen et al., 2006; Mai et al., 2009; Armon et al., 2015; Zhao et al., 2018). At depths of 30-36m, the more significant influence of sediments from the continent reduces the abundance and diversity of Foraminifera species.

*3.3.2. Delta front sandy - silty clay facies F3.2*

The delta front sandy-silty clay facies are distributed at depths between 11 m and 30 m. The main composition is thick brown silty clay and parallel, cross-bedding fine sand (Fig. 4, P5, P6, P7). The silty clay has an average particle size of 0.02-0.04 mm and a degree of sorting of 2.2-2.4. The fine sand has an average grain size of 0.06-0.07 mm and a degree of sorting of 2.3-2.6. In the cross-section, coarse grains gradually increase from bottom to top, and rare sediments with fragments of shells, due to stable dynamical conditions from waves and tides, are also observed. The results of radiocarbon dating $^{14}C$ at a depth of 20.5 m give the Age of 560 years cal BP. The abundant source of material from the continent brought out through the river mouth developed the pre-delta and greatly affected, and continues to affect, the living environment.

The sedimentary sets contain many fossils at depths from 24-27.6 m, 21-22 m, and 18-20 m, with typical species living in shallow seas identified, such as *Rotalidium annectent, Ammonia Rolshauseni, Cibicidoides lobatulus,* and *Ammonia pauciloculata* interspersed with sedimentary sets with no or scarce fossils at depths from 27.6-20 m, 22-24 m, 20-21 m, and 7-18 m. In these sedimentary sets, some sand shell species typical for coastal intertidal areas were identified, typically *Haplophragsmoides sp*., as well as some benthic shell species such as *Ammonia sp.* And *Quinqueloculina sp.* (Nguyen, 2006; Mai et al., 2009).

*3.3.3. Mouth bar sand facies F3.3*

Mouth bar sand facies are distributed at depths of 4-11 m, containing predominantly sand and poorly clayey silt. Sand particles are more frequent and coarser at the bottom than at the top. The average particle size is between 0.03 mm and 0.08 mm and a degree of sorting of 2-3.3. The upper part of the dune is mainly composed of sand containing many mica scales. The sediment has an obliquely layered structure (Fig. 4, P3, P4). The sediments are fossil-poor, with the number of individuals and the species composition being low, as well as tiny sizes of fossils with thin shell walls that are easy to break. *Quinqueloculina* sp., *Ammonia tepida,* and *Ammonia* sp. were found, both typical for estuarine environments, especially coastal tidal flats.

*3.3.4. Tidal flat clayey, silty sand facies F3.4*

Tidal flat facies are distributed at a depth of between 1.5 m and 4 m and are mainly composed of fine sand and brown, grayish-brown clay containing plant humus. The sediment structure shows thin interspersed diagonal layers, with an average particle size of 0.01-0.03 mm and a degree of sorting of 1.5-2.5. The sediments have many traces of biological activity, including plant roots and clay humus deposits (Fig. 4, P2), but are fossil-poor in terms of taxonomic composition (4 species). The typical species observed is *Ammonia tepida* - adapted to brackish water in coastal intertidal areas (Debenay et al., 1998, Nguyen, 2006).

*3.3.5. Delta plain silty clay facies F3.5*

The borehole is located in the coastal estuarine area, where the alluvium has only

formed recently. In addition, the artificial dike system has also blocked a significant portion of sediment delivery to the deltaic plain. Hence, the sediment layer is still relatively thin, with a 0 m to 1.5 m depth. The sediment is predominantly composed of brown silty clay with a thick layer structure (Fig. 4, P1), and the average particle size is between 0.01 mm and 0.02 mm, and the degree of sorting is 2.1-2.3. Rare deposits of shell fragments are also observed. No fossils were found in this facies.


*Figure 5*. Photos of Foraminifera fossils of the GAT borehole

a-e: *Ammonia tepida, Quinqueloculina* sp., *Quinqueloculina* sp. (*broken fossils are not intact*), *Haplophragsmoides* sp., and *Ammonia* sp.; f-j: *Hanzawaia nipponica, Rotalidium annectens, Quinqueloculina lamarkiana, Ammonia pauciloculata,* and *Cibicidoides wuellerstorfi;* k-o: *Textularia foliacea, Cibicidoides lobatulus, Biggenenrina nodosaria, Adelosina phillippinensis* (mature individuals reach large sizes), and *Globigerinoides* sp.; p-t: *Pseudorotalia indopacifica, Globigerinoides ruber, Amphistegina lessonii, Globigerinodies elongatus,* and *Siphonperta agglutinans*

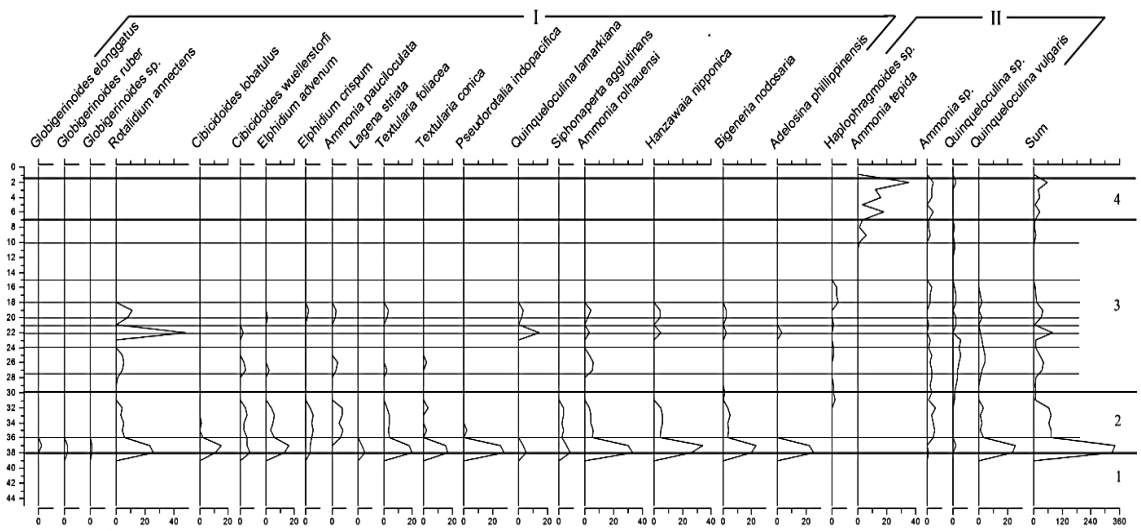


*Figure 6*. Distribution chart of Foraminifera fossils in GAT borehole
*I:* Group of fossils living commonly in shallow, coastal and offshore marine environments; *II:* The fossil group that commonly lives in the intertidal environment, in brackish water near the river mouth. 1, 2, 3, 4: Paleontological fossil zones

## 4. Discussions

The Pleistocene to Holocene sedimentary evolution in the Ba Lat river mouth (the Red River Delta) underwent three stages: the incised valley filled, estuarine, and deltaic.

### *4.1. The incised valley-filled stage*

The last glacial maximum was about 20000 years BP with a sea level of -120 m, followed by the Flandriand sea level rise, which was recorded by paleo-shoreline at depths of -50 m, -30 m, and -15 m at the respective times of 11,000, 10,000 and 9,000 years BP (Hanebuth et al., 2000), and the highest sea level rise reaches +2-3 m in the period 4000-6000 years BP (Lam and Boyd, 2001). The filling of incised valley occurred at the beginning of the Flandriand transgression by the river channel and floodplain sediment facies found in the GAT borehole at a depth of 54.5-70 m by dating of 1287 yr BP (Fig. 7).

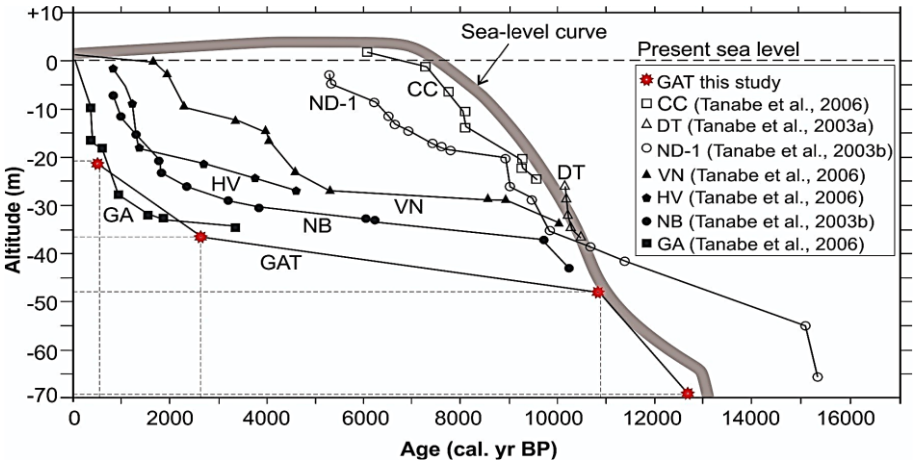


*Figure 7*. Accumulation curve of the core drill in the Red River Delta.
The sea level curve by Tanabe et al., 2003b

Based on the contour of the Groundwater table data, the line of the incised valley was sketched out by Tanabe (2006). However, the facies sediments at GAT, NP, and ND1 core indicate a new route of the incised valley (Fig. 8).

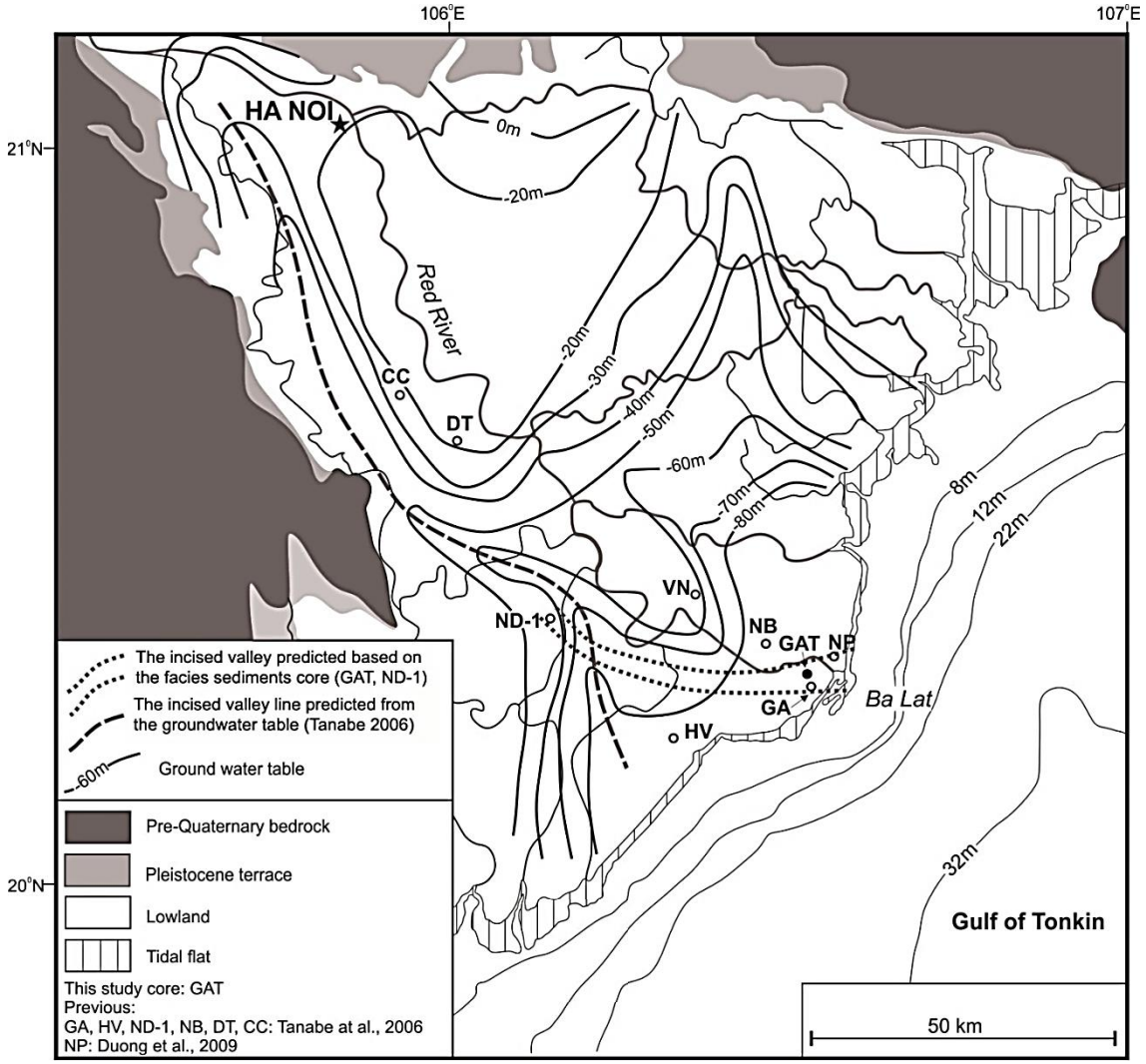


*Figure 8*. Sketch of incised valley route in the Red River Delta (modified after Tanabe et al., 2006)

The NP borehole (70 m depth) (Duong, 2009) is located on the other side of the Red River (about 8 km northeast of the GAT borehole). Holocene sediment in the NP borehole ends at 69.5 m depth. The NP borehole's cross-section has identified deltaic, estuarine, and filling incised valley facies. In contrast, the GAT borehole drilled to 70 m depth identified the incised valley sediment (from 54.5 m to 70 m depth). Therefore, the maximum depth of the incised valley sediment at the GAT borehole has not been determined.

In the Red River Delta, the ND1 borehole (Tanabe et al., 2003b) is located in the upper part of the Delta compared to the GAT borehole (40 km southwest). The incised valley sediment facies are distributed in the

ND1 and GAT boreholes at different depths (54-70 m and 54.5-70 m depths, respectively). The floodplain sediments are similarly distributed at differing depths in the ND1 and GAT boreholes (45-54 m and 52.4-54.5 m depths, respectively). This implies that the direction of the incised valley sediment from high to low parts is present at both ND1 and GAT boreholes. Moreover, the comparison between the GAT and NP boreholes shows that the riverbed at around 12,870 years BP was further to the west compared to where the Red River is now.

The channel of incised valley inclined towards the GAT borehole. In contrast, the NP borehole locates at the edge because the channel sediment facies were not found, only dawned floodplain facies at the NP core, whereas in GAT boreholes, both facies were found (Fig 9).

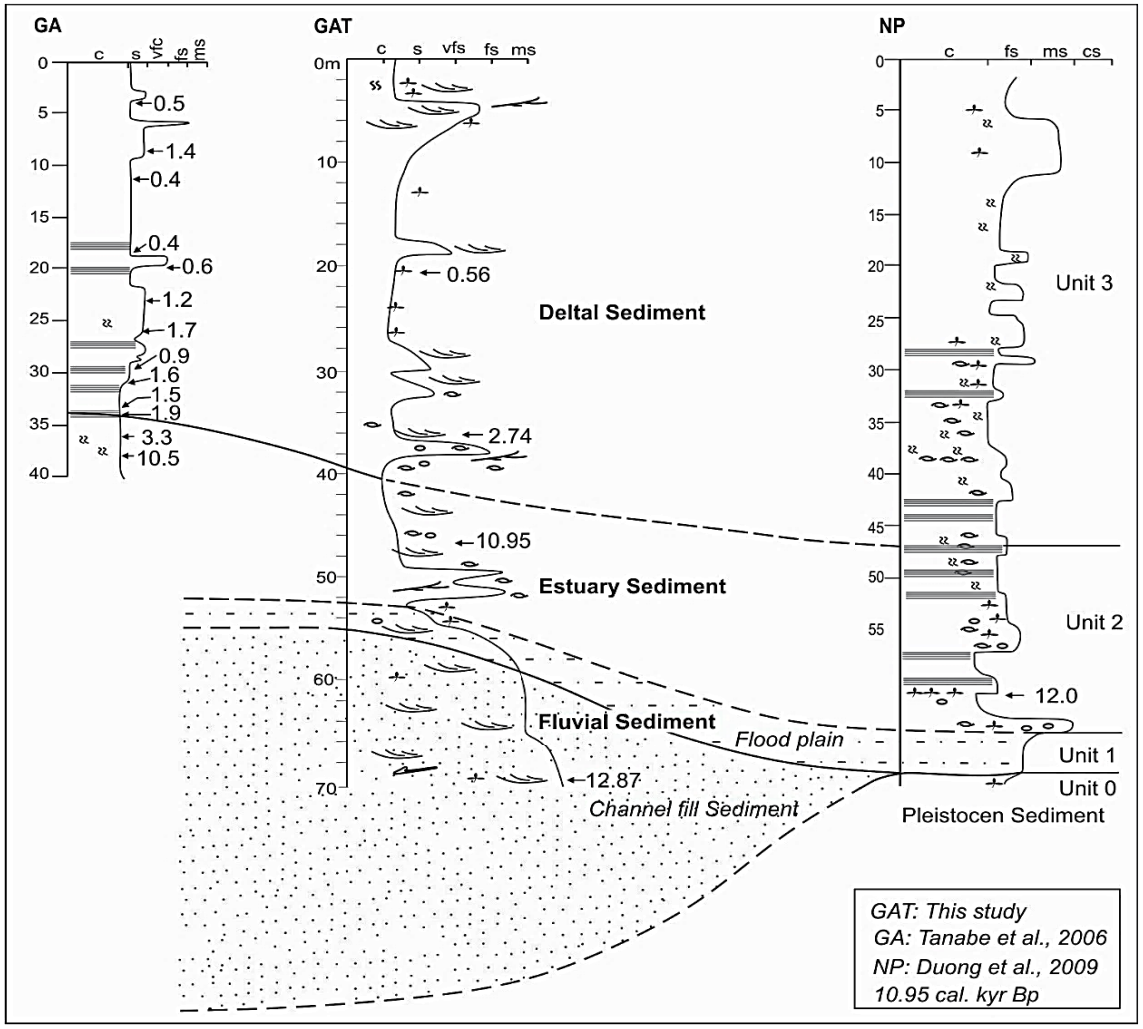


*Figure 9*. Cross-section of sediment facies in the Ba Lat river mouth

### *4.2. Estuarine stages*

Estuarine formations were found in the GAT borehole (38.0-52.5 m depth), including sedimentary facies such as tidal flat sands and bay clayey silt facies. Estuarine sediments are also found in the ND1, DT, CC, VN, GA, and

NB boreholes at 20.5-45.0 m; 22.6-41.3 m; 23.8-29.4 m; 36.6-40.2 m; 34.5-45.0 m depths, respectively (Tanabe et al., 2003b, 2006; Duong, 2009). As illustrated in the results, the estuarine sediments at the GAT borehole are distributed at the greatest depth (52.4 m depth). The $^{14}C$ Age of this sediment at 47.16 m depth is 10,950 yr BP, and the oldest ages at the ND-1, DT, CC, VN, GA, and NB boreholes are 11,400, 10,400, 9,500, 10,000, 10,500, and 10,200 yr BP, respectively (Tanabe et al., 2003b, 2006; Duong, 2009). Therefore, estuarine sedimentation likely began to form from 11,400 yr BP to 12,870 yr BP.

### *4.3. Deltaic stages*

Due to sea-level rise, the ocean moved further inland, reaching a high stand of 5-6 m above the present sea level, some 6,000-5,000 yr BP (Lam and Boyd, 2001). The Red River estuarine system has shown accumulation and widespread sediment dispersion. Therefore, accretion dominated and formed deltaic lobes, forming the Delta.

Most of the world's Holocene deltas began to form between 9,500 and 7,400 yr BP (Stanley and Warne, 1994). The Red River Delta began to form around 8,500 yr BP, as determined by the maximum flooding surface in the CC, DT, and ND2 core cross-sections (Hori et al., 2004). The Age of pro-delta sediments at the GAT core is 2,749 cal yr BP ($^{14}C$ analysis at 36.75 m depth). At this time, substantial accretion of deltaic facies began.

### *4.4. Sedimentation rate in the Ba Lat River mouth*

The sedimentation rate varies for each stage of delta evolution, which is apparent in the analyses of $^{14}C$ dating. The sedimentation stage resulted in rich sources of sediment from the continent depositing in the valley. In contrast, sea level rise accelerated the accretion of river beds and valleys. Results of the $^{14}C$ dating at depths of 69.51 m and 47.16 m give the corresponding ages of 12,870 BP and 10,950 years BP, respectively, with an average accretion rate of 11.64 mm/year (Fig. 10). During subsequent sea level rise, the Bay estuary was formed. The estuary moved further and further inland, with the location of the study area becoming an open sea area experiencing minor sediment accretion (as evidenced in the thin thickness of sediment in the GA core), with high rates of erosion caused by strong waves, (Tanabe et al., 2006). Comparing the results of absolute age analysis at a depth of 47.16 m and 36.75 m, the Age of 10,959 years BP and 2,740 years BP, respectively, show that the deposition rate in the open sea was shallow, reaching 1.27 mm/year.

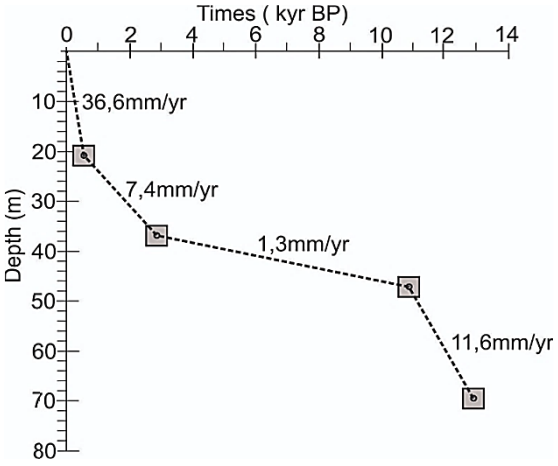


*Figure 10*. Sedimentation rate at the GAT borehole

## 5. Conclusions

The GAT borehole was taken at the Ba Lat river mouth, which belongs to the Red River Delta; based on the grain size distribution, foraminifera fossils, structure sediments, and $^{14}C$ dating, the Pleistocene - Holocene sediments were identified by 9 sedimentary facies, belonging to three groups: Incised valley facies (river channel sand facies, and floodplain clayey silt facies); Estuarine facies

(tidal flat sandy-silt facies, and bay clayey silt facies), and the deltaic facies (prodelta silty clay facies, delta front sandy-silty clay facies, mouth bar sand facies, tidal flats facies, and delta plain silty clay facies). The Age of the filled incised valley is 12,870 yr BP, while the estuarine clayey silt facies formed around 10,950 yr BP, and the pro-delta around 2,740 yr BP.

The presence of the incised valley and sediment-filling during the late Pleistocene to early Holocene at the site of the GAT borehole has been demonstrated by river channel and floodplain sediment facies dating to 12.870 yr BP. The location of the two boreholes (GAT and ND1) is oriented to determine the route of the cut valley in the Red River Delta.

The cross-section connecting NP, GAT, and GA boreholes in the Ba Lat estuary shows the river channel of the incised valley in the Late Pleistocene located southwest of the present Red River channel.

## Acknowledgments

The article was completed with the support of the basic investigation project "Investigating variation of the coastal plain for land use management in Nam Dinh and Ninh Binh provinces, Vietnam" (Code: UQDTCB.04/19-20) funded by VAST. The authors would like to sincerely thank the sponsors of the management agency and the agency in charge of the topic.

## References

Armon R.H., Hänninen O., 2015. Environmental indicators. Springer Dordrecht Heidelberg, 350p.

Davis R.A., 1992. Depositional Systems: An Introduction to Sedimentology and Stratigraphy. Prentice Hall, 634p.

Debenay J.-P., 2012. A Guide to 1,000 Foraminifera from Southwestern Pacific: New Caledonia. IRD Editions, 385p.

Debenay J.-P., Bénéteau E., Zhang J., Stouff V., Geslin E., Redois F., Fernandez-Gonzalez M., 1998. Ammonia beccarii and Ammonia tepida (Foraminifera): morphofunctional arguments for their distinction. Mar. Micropaleontol, 34, 235-244.

Doan Thi O., Duong Thi T., Nguyen Thi Nhu H., Hoang Thi Q., Le Thi Phuong Q., Duong Hong P., Le Phuong T., Bui Huyen T., 2021. Preliminary results on microplastics in surface water from the downstream of the Day River. Vietnam J. Earth Sci., 43(4), 485-495. https://doi.org/10.15625/2615-9783/16504.

Duong N.T., 2009. Palynological investigation from a deep core at the Coastal area of the Red River Delta, Vietnam. VNU J. Sci. Earth Environ. Sci., 25, 192-203.

Duong N.T., Lieu N.T.H., Cuc N.T.T., Saito Y., Huong N.T.M., Phuong N.T.M., Thuy A.T., 2020. Holocene paleoshoreline changes of the Red River delta, Vietnam. Rev. Palaeobot. Palynol, 278, 104235.

Fan D., 2012. Open-coast tidal flats. Princ. Tidal Sedimentol, 187-229.

Funabiki A., Haruyama S., Van Quy N., Van Hai P., Thai D.H., 2007. Holocene delta plain development in the Song Hong (Red River) delta, Vietnam. J. Asian Earth Sci., 30, 518-529.

Gallagher S.J., Wallace M.W., Li C.L., Kinna B., Bye J.T., Akimoto K., Torii M., 2009. Neogene history of the West Pacific warm pool, Kuroshio and Leeuwin currents. Paleoceanography, 24, PA1206. Doi.org/10.1029/2008PA001660.

Hai N.M., Ouillon S., Vinh V.D., 2022. Sea-level rise in Hai Phong coastal area (Vietnam) and its response to ENSO-evidence from tide gauge measurement of 1960-2020. Vietnam J. Earth Sci., 44(1), 109-126.

Hanebuth T., Stattegger K., Grootes P.M., 2000. Rapid Flooding of the Sunda Shelf: A Late-Glacial Sea-Level Record. Science, 288, 1033-1035.

Hanebuth T.J.J., Saito Y., Tanabe S., Vu Q.L., Ngo Q.T., 2006. Sea levels during late marine isotope stage 3 (or older?) reported from the Red River delta (northern Vietnam) and adjacent regions. Quat. Int., Quaternary sea-level changes: contributions from the 32nd IGC 145-146, 119-134. https://doi.org/10.1016/j.quaint.2005.07.008.

Hoan H.V., Larsen F., Pham Quy N., Tran Vu L., Nguyen Thi Thanh G., 2022. Recharge

mechanism and salinization processes in coastal aquifers in Nam Dinh province, Vietnam. Vietnam J. Earth Sci., 44(2), 213-238. https://doi.org/10.15625/2615-9783/16864.

Hoang Van L., Nguyen Tien T., Vu Tat T., Nguyen Thanh T., Nguyen Lam A., Dao Bui D., Le Van D., Tran Ngoc D., Nguyen Huu H., 2021. Holocene sedimentation offshore Southeast Vietnam based on geophysical interpretation and sediment composition analysis. Vietnam J. Earth Sci., 43(3), 336-379. https://doi.org/10.15625/2615-9783/16268.

Hori K., Tanabe S., Saito Y., Haruyama S., Nguyen V., Kitamura A., 2004. Delta initiation and Holocene sea-level change: example from the Song Hong (Red River) delta, Vietnam. Sediment. Geol., 164, 237-249. https://doi.org/10.1016/j.sedgeo.2003.10.008.

Lac M.V., Thu V.A., Thuoc D.T.B., 2009. Ecological and evolutionary divergence of Foraminifera in the Gulf of Tonkin. Vietnam J. Earth Sci., 31(2), 139-147.

Lam D.D., Boyd W.E., 2001. Some facts of sea-level fluctuation during the Late Pleistocene-Holocene in HaLong Bay and Ninh Binh area (in Vietnam). Vietnam J. Earth Sci., 23(1), 86-91.

Le Duc L., Nguyen H., Shinjo R., B. Shakirov R., Obzhirov A., 2021. Chemical, mineralogical, and physicochemical features of surface saline muds from Southwestern sub-basin of the East Vietnam Sea: Implication for new peloids. Vietnam J. Earth Sci., 43(4), 496-508. https://doi.org/10.15625/2615-9783/16561.

Le N.D., Hoang T.T.H., Duong T.T., Phuong N.N., Le P.T., Nguyen T.D., Phung T.X.B., Le T.M.H., Le T.L., Vu T.H., Le T.P.Q., 2022. Microplastics in the Surface Sediment of the main Red River Estuary. Vietnam J. Earth Sci., 45(1), 19-32. https://doi.org/10.15625/2615-9783/17486.

Lei Y., Li T., 2016. Atlas of benthic Foraminifera from China seas: The Bohai Sea and the Yellow Sea. Springer Geology, 399p. Doi: 10.1007/978-3-662-53878-4.

Li Shunli, Li Shengli, Shan X., Gong C., Yu X., 2017. Classification, formation, and transport mechanisms of mud clasts. Int. Geol. Rev., 59, 1609-1620. https://doi.org/10.1080/00206814.2017.1287014.

Luu T.T., Hien N.T.T., 2022. Rooftop rainwater harvesting and artificial groundwater recharge-a case study: Thanh Xuan district in south of Hanoi. Vietnam J. Earth Sci., 44(2), 286-300.

McGowen J.H., Garner L.E., 1970. Physiographic Features and Stratification Types of Coarse-Grained Pointbars: Modern and Ancient Examples1. Sedimentology, 14, 77-111. https://doi.org/10.1111/j.1365-3091.1970.tb00184.x.

Milliman J.D., Syvitski J.P., 1992. Geomorphic/tectonic control of sediment discharge to the ocean: the importance of small mountainous rivers. J. Geol., 100, 525-544.

Nghi T., Toan N.Q., 2000. Development history of deposits in the Quaternary of Vietnam. Weather. Crust Quat. Sediments Vietnam Dep. Geol. Miner. Vietnam, Hanoi, 177-192.

Ngoc N., Cu N.H., Bat D., 2006. Cenozoic Foraminifera in the shelf and adjacency of Vietnam, VAST, 392p.

Nichols G., 2009. Sedimentology and Stratigraphy. John Wiley & Sons, 419p.

Reimer P., et al., 2020. The IntCal20 Northern Hemisphere Radiocarbon Age Calibration Curve (0-55 cal kBP). Radiocarbon, 62(4), 725-757. Doi: 10.1017/RDC.2020.41.

Reymond C.E., Mateu-Vicens G., Westphal H., 2014. Foraminiferal assemblages from a transitional tropical upwelling zone in the Golfe d'Arguin, Mauritania. Estuar. Coast. Shelf Sci., 148, 70-84. https://doi.org/10.1016/j.ecss.2014.05.034.

Stanley D.J., Warne A.G., 1994. Worldwide Initiation of Holocene Marine Deltas by Deceleration of Sea-Level Rise. Science, 265, 228-231. https://doi.org/10.1126/science.265.5169.228.

Tanabe S., Hori K., Saito Y., Haruyama S., Kitamura A., 2003a. Song Hong (Red River) delta evolution related to millennium-scale Holocene sea-level changes. Quat. Sci. Rev., 22, 2345-2361.

Tanabe S., Hori K., Saito Y., Haruyama,S., Sato,Y., Hiraide S., 2003b. Sedimentary facies and radiocarbon dates of the Nam Dinh-1 core from the

Song Hong (Red River) delta, Vietnam. J. Asian Earth Sci., 21, 503-513.

Tanabe S., Saito Y., Vu Q.L., Hanebuth T.J., Ngo Q.L., Kitamura A., 2006. Holocene evolution of the Song Hong (Red River) delta system, northern Vietnam. Sediment. Geol., 187, 29-61.

Thanh N.T., Liu P.J., Dong M.D., Nhon D.H., Cuong D.H., Dung B.V., Van Phach P., Thanh T.D., Hung D.Q., Nga N.T., 2018. Late Pleistocene-Holocene sequence stratigraphy of the subaqueous Red River delta and the adjacent shelf. Vietnam J. Earth Sci., 40(3), 271-287.

Zhao B., Yan X., Wang Z., Shi Y., Chen Z., Xie J., Chen J., He Z., Zhan Q., Li X., 2018. Sedimentary evolution of the Yangtze River mouth (East China Sea) over the past 19,000 years, with emphasis on the Holocene variations in coastal currents. Palaeogeogr. Palaeoclimatol. Palaeoecol., 490, 431-449.